DIRECT DETERMINATION OF THE CALCIUM PROFILE STRUCTURE FOR DIPALMITOYLLECITHIN MULTILAYERS USING NEUTRON DIFFRACTION

L. HERBETTE, C. A. NAPOLITANO, AND R. V. MCDANIEL
Departments of Medicine and Biochemistry, University of Connecticut Health Center, Farmington, Connecticut 06032; and Brookhaven National Laboratory, Biology Department, Upton, New York 11973

ABSTRACT The distribution of calcium in lamellar phases of dipalmitoyllecthin (DPPC) multilayers was directly determined by neutron diffraction and stable isotope substitution of ^{44}Ca for ^{40}Ca. A significant resonance effect on the intensities of the lamellar diffraction pattern was observed for millimolar concentrations of these calcium isotopes. The calcium difference profile indicated that calcium was localized in the phospholipid headgroup region, being excluded from the hydrocarbon core as was water separately determined from the water profile structure obtained by H_2O/D_2O exchange. A reciprocal space analysis of the difference structure factors indicated that calcium binds preferentially to within 1–2 Å of the phosphate moiety of the phospholipid head groups of the DPPC bilayer.

INTRODUCTION

The interaction of calcium ions with phosphatidylcholine bilayers, examined by several investigators using electrophoretic (1) and x-ray diffraction (2) techniques, indicates that calcium ions are absorbed to zwitterionic lipid head groups. Theoretical arguments based on electrostatic double-layer theory have assumed there is a calcium binding plane 3.5 Å from a hypothetical interface that separates water from lipid bilayers (3); however, the site of such adsorption has never been directly determined. Direct methods using hydrogen-deuterium exchange and neutron diffraction have allowed small molecules such as hexane (4) and drugs (5) to be localized in model membrane systems, and have provided information regarding the conformation of lipid molecules in model membranes (6, 7) and the conformation and distribution of lipids in reconstituted biological membranes (8, 9) and isolated membranes (10). When coupled to x-ray diffraction measurements, neutron diffraction can also be used to locate protein, lipid, and water components in biological membranes.

In the present study, the first direct localization of calcium in lamellar phases of dipalmitoyllecithin (DPPC) multilayers was achieved by stable isotope substitution of ^{44}Ca and ^{40}Ca in a neutron diffraction study at 15 Å resolution (four diffraction orders of a 60-Å repeat). This is possible because the coherent neutron-scattering cross section is different for ^{40}Ca (0.49×10^{-13} cm) and ^{44}Ca (0.18×10^{-13} cm) (11), which creates measureable contrast for millimolar Ca^{2+} concentrations. Using a theoretical calculation of difference structure factors as a function of the molar ratio of calcium bound to DPPC the experimentally determined molar ratio was predicted to within experimental error. A reciprocal space model refinement analysis operating on the experimental difference structure factors (6) provided both the mean position and distributional width for the real space calcium peak densities to within 1 Å along the profile axis. A comparison of the calcium difference profile with the water profile structure and electron density profile of DPPC showed that calcium is localized preferentially within the phospholipid head group region of the DPPC bilayer and is probably bound to the phosphate moiety within the head group.

MATERIALS AND METHODS

1–2 mg of anhydrous ^{40}calcium carbonate (Mallinckrodt Inc., Science Products Div., St. Louis, MO; analytical reagent grade, 100 mol wt) or ^{44}calcium carbonate (Merck Chemical Div., Merck and Co., Inc. Isotopes, Montreal, Canada; MH-2490, 98.68 atm percent ^{44}Ca, mol wt 104) was added to 5 or 10 μl of 12 N HCl plus 1.0 ml of glass distilled water. After incubating at 85°C for 60 min, cooling to room temperature, and neutralizing with NaOH, 1.0 ml of Tris buffer (10 mM, final pH 7.2) 2.0 mg L-α-dipalmitoylphosphatidylcholine (DPPC; Calbiochem-Behring Corp., La Jolla, CA or Sigma Chemical Co., St. Louis, MO) were added for neutron diffraction studies. For x-ray diffraction, 0.5 mg DPPC was added to this buffer containing calcium. The lipid/buffer suspension was sonicated for 60 s at low power with a microtip sonifier (Branson Sonic Power Co., Danbury, CT) with heating above the lipid phase transition temperature. The final concentration of calcium in the DPPC dispersion was 5 or 10 mM. Henceforth, 5 mM Ca and 10 mM Ca will refer to the concentrations of calcium before centrifugation of the DPPC dispersion. The DPPC dispersion was placed in plexiglas sedimentation cells (12) and centrifuged in a SW27 rotor (Beckman Instruments, Inc., Fullerton, CA) at 25,000 rpm for 60 min producing either a 0.5- or 1-cm diameter pellet on aluminum foil. The aluminum foil was mounted on curved (for x-ray diffraction) or flat (for neutron diffraction) glass plates and equilibrated

with an atmosphere of 66% relative humidity (over saturated sodium nitrate) or 81% relative humidity (over saturated ammonium nitrate) at 10 ± 2°C for 24–48 h. For some neutron diffraction experiments, the saturated salt solutions were made up in 10% (vol/vol) deuterium oxide.

The molar ratio of calcium to phospholipid was determined in preparations of DPPC multilayers containing ^{45}Ca. The amount of radiolabeled calcium in the DPPC multilayer was determined by standard scintillation procedures. The total phospholipid was determined by weighing DPPC multilayers that had been placed over a dessicant and dried in an oven at 75°C. The total phospholipid recovery was >95%. These measurements gave a ratio of 10 ± 1 mol phospholipid/mol calcium at the 5-mM initial calcium concentration used in the neutron diffraction study. The water content of the DPPC multilayers partially dehydrated at 66% relative humidity was determined by adding a ^3H_2O tracer to the saturated salt solution. The DPPC multilayer was allowed to equilibrate in a chamber sealed with a rubber stopper containing the radiolabeled atmosphere. After partial dehydration, scintillation fluid was quickly added through a syringe to the multilayer sample within the sealed chamber, after which the sample was immediately removed from the radiolabeled atmosphere and counted for ^3H. The water content of the multilayer measured in this manner was 0.37 ± 0.03 μl/2 mg DPPC. This water content was equivalent to 7.5 ± 1.0 mol water/mol phospholipid.

X-ray diffraction patterns (meridional reflections of oriented lamellar samples) were recorded on no-screen x-ray film (Eastman Kodak Co., Rochester, NY) during exposures of 2–9 h using a toroidal mirror assembly in a Searle x-ray diffraction camera (Baird and Tatlock, Romford, England) and a Spectra fixed anode generator (Spectra Equipment Corp., North Royalton, OH) generator or using Franks' optics on a Rigaku-Denki (model RU3; Rigaku/USA Inc., Danvers, MA) rotating anode generator (CuKα radiation, λ = 1.54 Å with $K_{\alpha 1}$ and $K_{\alpha 2}$ being unresolved). The optical density of the films was measured with a Quick Scan R&D densitometer (Helena Laboratories, Beaumont, TX) with an integrating slit beam height made a factor of five or more smaller than the height of the full extent of the lamellar reflections. A 10/1 reduction in scan speed (compared with the original specifications) allowed slow scanning through the center of each lamellar reflection arc. The background subtracted intensity function contained four diffraction orders and was corrected by $s^2 = (h/d)^2$ as previously described (13). In this correction, one factor of s arises from the intersection of the reciprocal lattice for the cylindrically curved multilayer specimen with the Ewald sphere and the other is caused by the arcing of the reflections on the surface of the Ewald sphere due to mosaic spread of the multilayer. Structure factors derived from these intensity amplitudes were independently phased by the swelling method (14) using an algorithm (15) as previously described (13). Unit cell electron density profile structures were calculated from the appropriately corrected and phased structure factors by a Fourier series approximation.

Neutron diffraction patterns were recorded on a two-dimensional position-sensitive gas flow detector at the high flux beam reactor facility of Brookhaven National Laboratories (Upton, NY) as previously described (13). A planar sample was rotated ($0° \le \omega \le 6°$; $\Delta\omega = 0.1°$) about the ω-axis, which is defined as the axis perpendicular to both the neutron beam and the sedimentation axis of the multilayer sample, and the entire lamellar reflection arc for $h = 1$–4 was recorded on the two-dimensional detector. Point-to-point subtraction of scattering by a lipid-free aluminum foil/glass substrate from each neutron diffraction pattern yielded a background-corrected lamellar intensity function in which each lamellar reflection was numerically integrated over a width (along the lamellar meridional axis) of 14 detector channels. The integrated intensities were corrected by one factor of $s = h/d$ because the lamellar neutron reflections were integrated over the full extent of the reflection arc collected on the face of the two-dimensional counter in contrast to the data reduction methods in x-ray diffraction studies. The origins of the different correction factors for x-ray and neutron diffraction have been justified previously (12, 13). Error ranges for the structure factors given in Table I were calculated as described in Eq. A1 of the Appendix using:

$$N = \left(\sum_{k=1}^{7} \sum_{i=m(2h-1)/2}^{hm-b} |I(i) - I(i+k)| + \sum_{k=1}^{7} \sum_{i=hm+b}^{m(2h+1)/2} |I(i) - I(i+k)| \right) / \Delta. \quad (1)$$

Operationally, a value of $k = 7$ was used because for $k \ge 6$ the value of N was constant, whereas for $k = 1$–5 the value of N fluctuated. This was reasonable because the channel-to-channel noise was determined to be random and not correlated so that averaging over several different

TABLE I

STRUCTURE FACTORS FOR NEUTRON SCATTERING BY DPPC MULTILAYERS IN 5 mM ADDED ^{44}Ca OR ^{40}Ca IN 100% H_2O AND 10% D_2O

Isotope	Scattering amplitude density*	Order‡	Structure factor		Phase (φ)
			100% H_2O	10% D_2O	
	10^{-14} cm/Å^3		$d = 59.10$ Å	$d = 59.42$ Å	
^{40}Ca	11.7	1	93.6 ± 0.7	116.8 ± 0.7	π
		2	42.5 ± 3.3	34.5 ± 4.5	π
		3	65.1 ± 5.4	62.2 ± 5.0	0
		4	38.9 ± 9.8	28.1 ± 12.0	π
			$D = 60.95$ Å	$D = 60.33$ Å	
^{44}Ca	4.5	1	83.2 ± 0.8	100.0 ± 0.4	π
		2	45.3 ± 3.0	33.7 ± 2.2	π
		3	62.5 ± 3.3	56.6 ± 3.5	0
		4	31.0 ± 9.4	—	π
D_2O	6.3	—	—	—	—
H_2O	−0.6	—	—	—	—

Error ranges were calculated as in Materials and Methods.

*Scattering amplitude densities were calculated from the atomic volumes of calcium isotopes and the scattering lengths, $b(^{40}Ca) = 0.49 \times 10^{-13}$ cm and $b(^{44}Ca) = 0.18 \times 10^{-13}$ cm (11).

‡$I(h = 5)$ was not used in the analysis for Figs. 2–3 because the phase factor (φ) was not unambiguously determined. (Results using $I[h = 5]$ assuming $\phi = \pi$ as discussed are given later in Fig. 4.)

channel differences yielded a smoothed average value of N. Structure factors in Table I were calculated from $\sqrt{h/d \cdot I(h/d)}$.

Experiments including H_2O/D_2O exchange were carried out on the same sample. Structure factors as given in Table I arising from different samples containing either ^{40}Ca or ^{44}Ca were scaled to one another by the difference structure factors from H_2O/D_2O exchange according to Buldt et al. (6). Structure factors were corrected for small differences in lamellar spacings between samples containing different isotopes of calcium (<1–2 Å) and for samples that underwent H_2O/D_2O exchange (<0.6 Å)[1] by using the sampling theorem application of the minus fluid model (16) according to Buldt (see Eq. 4 of reference 6). The zero-order intensity was estimated from the equation (16)

$$I_{cal}(h = 0/d) = 2\int_0^{\nu} [P(x) - P(\nu)]\, dx, \qquad (2)$$

where P is the Patterson function obtained from the observed intensities, d is the unit cell repeat distance, and ν is the membrane width extent as defined by $d = 2dw + \nu$, where dw equals the pure water layer extent near $\pm d/2$ of the unit cell. The value of $\nu = 49$ Å was obtained from Buldt et al. (6) for DPPC in the $L_{\beta'}$ phase. Because the average neutron-scattering amplitude density for the membrane is greater than that for water, the zero-order structure factor obtained from $I_{cal}(h = 0/d)$ is positive and this value was used in the sampling theorem correction for different lamellar spacings. These corrected structure factors for ^{40}Ca vs. ^{44}Ca in 100% H_2O are given in Table II.

All structure factor data sets derived from neutron-diffraction intensities were independently phased by the swelling method (14) using an algorithm (15) as previously described (13). Difference Fourier transforms were thus derived from the appropriately corrected, scaled, and phased structure factors for ^{40}Ca-DPPC and ^{44}Ca-DPPC as previously described (8). The model of the calcium difference profile was refined by following the reciprocal space procedure of Buldt et al. (6) (assuming a Gaussian distribution for the calcium isotopes along the profile axis). This model was deemed reasonable after inspecting the real-space difference profiles. This approach was used to avoid resolution limitations in extracting information from experimentally derived difference profiles. Specifically, the unit cell calcium difference profiles contained two maxima and could be described by a Gaussian distribution:

$$g(x) = \frac{1}{\nu\sqrt{\pi}} \{e^{-[(x-x_0/\nu)]^2} + e^{-[(x+x_0/\nu)]^2}\}, \qquad (3)$$

where ν is the $1/e$ half-width and x_0 is the mean position for describing these difference profile maxima. This Gaussian distribution was Fourier transformed to provide calculated difference structure factors, $F_c(h)$, which were fitted to the experimental difference structure factors, $F_e(h)$, in a least-squares calculation for the parameters ν and x_0 according to

$$\Sigma |F_e(h) - AF_c(h)|^2 \rightarrow \min, \qquad (4)$$

where

$$A = \sum_h |F_e(h)| \Big/ \sum_h |F_c(h)|. \qquad (5)$$

In practice, the mean position (x_0) for the calcium difference maxima could be determined to less than ±1 Å using this model refinement approach when the least-squares fit for the calculated and experimental structure factors was compared with the noise of the experimental structure factors. The model refinement calculation was found to be less sensitive to the Gaussian half-width parameter (ν) and could be determined to about ±1 Å. The advantages and specific limitations of this model refinement procedure have been described elsewhere in detail (6–8).

[1]This correction for samples that underwent H_2O/D_2O exchange (d-spacing differences that were <0.6 Å) was very small because the H_2O/D_2O exchange was performed on the same sample. The corrected structure factors in 10% D_2O are thus omitted in Table II. The water profile structure given in Fig. 3 *B* was, however, derived from the appropriately corrected structure factors even though this correction was small. For different samples, the d-spacing differences were on the order of 1–2 Å and this correction was significant as indicated by comparing Tables I and II.

TABLE II
STRUCTURE FACTORS CORRECTED FOR SMALL DIFFERENCES IN LAMELLAR SPACING

Order	Structure factor (100% H_2O)	
	^{40}Ca d = 60.95 Å	^{44}Ca d = 60.95 Å
1	−89.6 ± 0.7	−83.2 ± 0.8
2	−54.2 ± 4.2	−45.3 ± 3.0
3	68.5 ± 5.7	62.5 ± 3.3
4	−31.0 ± 7.8	−31.0 ± 9.4
5*	(10.0)	(12.9)

*Indicated for purposes of calculating profile structures of Fig. 4 to compare with those given in Figs. 2 and 3. Average amplitude is given; phase factor not determined (see text).

RESULTS AND DISCUSSION

The relative intensities of the lamellar reflections $[I(h = 1)–I(h = 4)]$ were found to be sensitive to the calcium isotopes, at concentrations of 5 and 10 mM. Fig. 1 shows the unscaled background-corrected neutron-scattering intensity as a function of scattering angle for DPPC multilayers in 100% H_2O with 10 mM ^{40}Ca or ^{44}Ca. This inability to superimpose the first four diffraction orders arising from different DPPC multilayer samples containing different calcium isotopes in 100% H_2O clearly demonstrates that a multiplicative factor is absent that could equate the entire lamellar intensity function over this region of reciprocal space ($0 \leq s \leq 0.075$ Å^{-1}). Thus, these differences in lamellar intensities must partly result from the presence of different calcium isotopes. Table I gives the scaled structure factors for a DPPC multilayer (5 mM ^{40}Ca and ^{44}Ca) in 100% H_2O and 10% D_2O. Scaled structure factors for DPPC with ^{40}Ca and ^{44}Ca (5 mM) in 100% H_2O, appropriately corrected for small differences in the lamellar spacings arising from different samples (Table II), were used in generating Figs. 2, 3 *C*, 4 *B* and 4 *C*. The scaling factor (S) used to equate the structure factors from different samples in Tables I and II was equal to 1.5 such that for the ^{40}Ca data, $F(h) = (1.5) \cdot F'(h)$, where $F'(h)$ are the experimentally obtained structure factors. S, which corrects for differing neutron beam intersections with differing amounts of (lipid/water) sample, is calculated as the ratio of the summed difference structure factors for 10% D_2O vs. 100% H_2O between samples with different calcium isotopes (6). Because of uncertainty in the intensities of weak orders e.g., see noise level in Fig. 1 and error ranges in Table I), the value of S has an error range of ±0.1 for the 5 mM Ca results. However, the

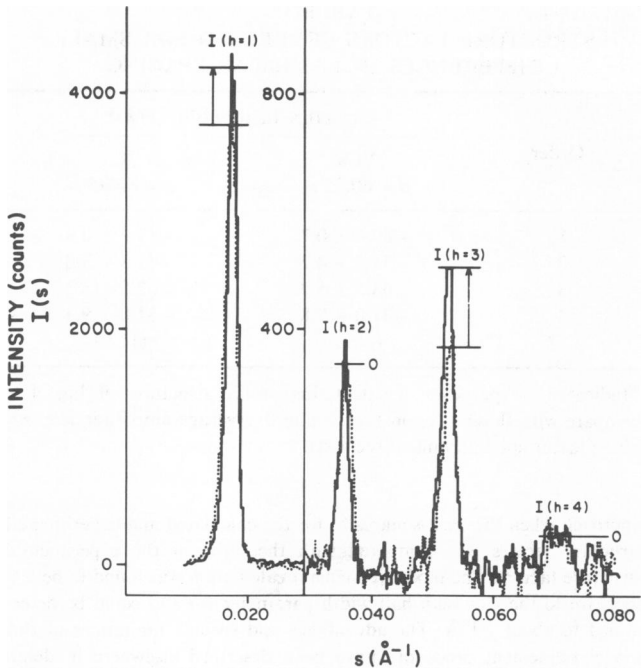

FIGURE 1 Background-corrected neutron-scattering intensity as a function of the reciprocal space coordinate, s (0.010 $Å^{-1} \leq s \leq 0.080$ $Å^{-1}$), is shown for DPPC multilayers in 10 mM added ^{40}Ca (dotted line) or ^{44}Ca (solid line) in 10% D_2O at 10°C. Second-, third-, and fourth-order reflections are expanded fivefold on the $I(s)$-axis. Arrows on $I(h = 1$ and 3) represent the changes in scattering intensity for different samples with ^{40}Ca vs. ^{44}Ca. Zeroes on $I(h = 2$ and 4) represent the intensities that were unchanged within the noise level. Note that there is no multiplicative factor for these two intensity functions that can eliminate the intensity differences that must be, in part, caused by isotope substitution (see text and Table II).

choice of S does not qualitatively alter the calcium difference profiles over this uncertainty range, which indicates that the calcium density is higher toward the extremes ($\pm d/2$) of the unit cell than in the central hydrocarbon region as illustrated in Fig. 2. Fig. 2 *A–D* provides the profiles obtained using S values of 1.4, 1.5, 1.6, and 1.7, respectively, at 15-Å resolution (four diffraction orders of a 60-Å repeat). An indication that S = 1.5–1.6 is the correct choice for the scale factor comes from comparing Figs. 2 *A–D*. The Fourier ripple in the central hydrocarbon region of the bilayer oscillates about the actual calcium density, which should be zero and constant if divalent cations are excluded from the hydrocarbon core. This condition is most closely approached in Fig. 2 *B* or *C*, with S = 1.5–1.6, whereas other choices of S give either a central peak (Fig. 2 *A*) or trough (Fig. 2 *D*) in average calcium density (compare dotted lines drawn through the Fourier ripple in Fig. 2 *A–D*).

The difference in the structure factors for ^{40}Ca vs. ^{44}Ca as given in Table II are significant and can be shown within experimental error to arise from the difference in scattering lengths of these two calcium isotopes. For the 5-mM calcium DPPC multilayer samples, assays for calcium and phosphate showed that the DPPC multilayer contained 10 ± 1 mol phospholipid/mol calcium. Using calculated scattering amplitude densities for the calcium isotopes, water, and DPPC, the calculations presented in the Appendix showed that for calcium bound to the phospholipid head group region of the DPPC lipid bilayer, the experimentally determined difference structure factors should correspond to a difference (unit cell) profile where 1 mol calcium is bound to 11 mol phospholipid. This calculated

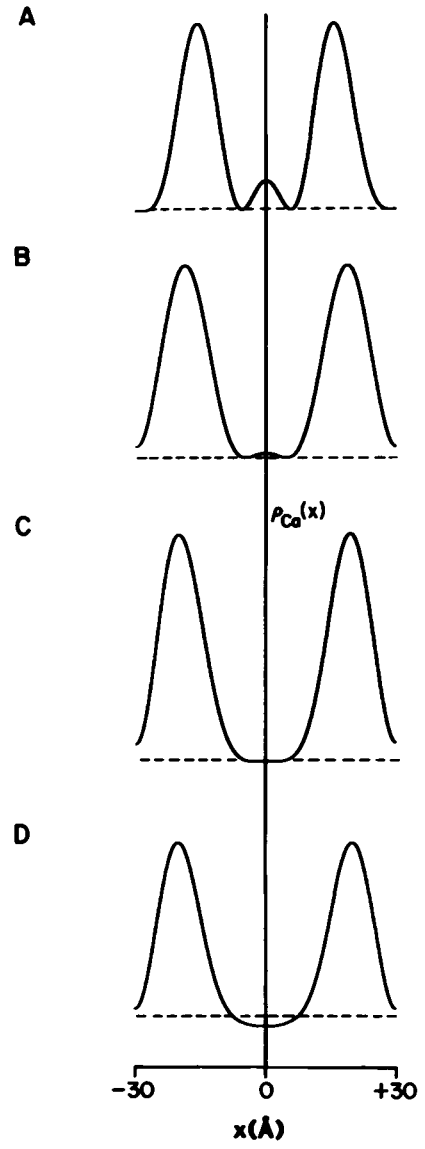

FIGURE 2 Calcium difference profiles for DPPC bilayers at 10°C in 5 mM added ^{40}Ca vs. ^{44}Ca are shown. x represents the distance from the bilayer center in ångströms (Å). The resolution is 15 Å (four orders). The neutron density of the ^{44}Ca sample was subtracted from the scaled neutron density of the ^{40}Ca sample with the following scale factors (S): (*A*) S = 1.4, (*B*) S = 1.5, (*C*) S = 1.6, and (*D*) S = 1.7. The dotted lines in *A–D* represent the average calcium density in the hydrocarbon region of the bilayer. At S = 1.5–1.6, the average density is constant in the hydrocarbon core, as expected if $\rho_{Ca}(x) = 0$ throughout this region.

molar ratio (11/1) is within the standard deviation of the experimentally determined ratio of 10 ± 1 mol phospholipid/mol calcium.

Fig. 3 *A–D* shows the 15-Å resolution profiles of the neutron-scattering density of ^{40}Ca-DPPC in 100% H_2O, the water distribution from H_2O/D_2O exchange, the calcium distribution from 5 mM calcium isotope replacement, and the electron density distribution from 5 mM ^{40}Ca-DPPC, respectively. All profiles illustrated in Fig. 3 were calculated using four diffraction orders of a 60-Å repeat. The major maxima in the neutron density profile and electron density profile, which are separated by 42 and 45 Å, respectively, correspond to the average positions of the phospholipid head groups in each monolayer of a bilayer unit cell. The central troughs in neutron and electron density correspond to the location of methyl groups at the center of each bilayer with somewhat higher density occurring for the methylene chains. Major maxima occur in the calcium difference profile (Fig. 3 *C*) near the edges of the unit cell (near $X = \pm d/2$) and are within the plane of the maxima corresponding to the phospholipid head groups of each monolayer of the bilayer unit cell. The low calcium content within the hydrocarbon core region is especially evident when the water (Fig. 3 *B*) and calcium (Fig. 3 *C*) difference profiles are compared. These features of the difference calcium profile indicate that calcium is excluded from the hydrocarbon core region of the bilayer and is present, instead, in a region containing water.

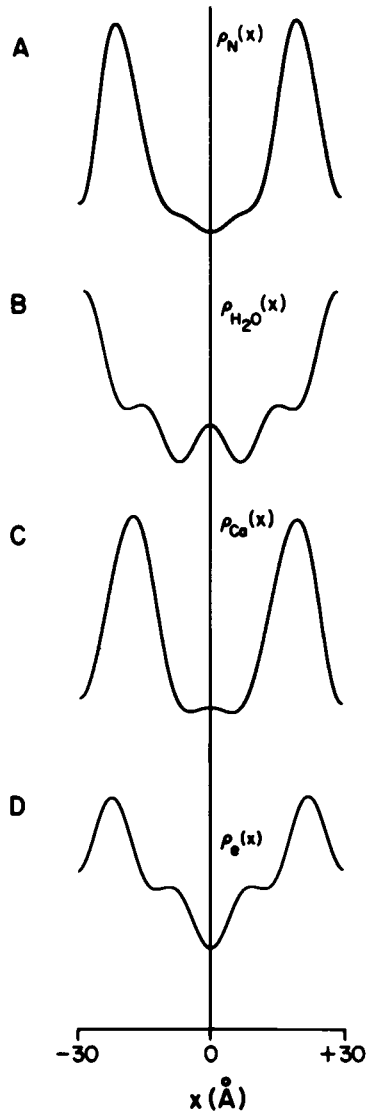

FIGURE 3 Density profiles for DPPC bilayers at 10°C in 5 mM added ^{40}Ca or ^{44}Ca are presented. x represents the distance from the bilayer center in ångströms. The resolution is 15 Å (four orders). (*A*) The neutron scattering density of the ^{40}Ca sample in 100% H_2O is shown. (*B*) The water difference profile of ^{40}Ca sample is shown. Neutron-scattering density in 100% H_2O was subtracted from neutron-scattering density in 10% D_2O. The water difference profile for the ^{44}Ca sample (not shown) was similar to that for the ^{40}Ca sample. (*C*) The calcium difference profile of the 100% H_2O sample with the ^{44}Ca neutron-density subtracted from the scaled ^{40}Ca neutron density is shown. The scaling factor (*S*) is 1.5. (*D*) The electron density of a separate sample that was made in 5 mM added ^{40}Ca is shown, as derived from x-ray diffraction.

At 15-Å resolution, the major maxima within the calcium difference profile structure appear symmetric. The fifth-order lamellar reflection (Table II) was used to discern the shape of these maxima at higher resolution where $|F(h = 5)|$ equals 10.0 and 12.9 for ^{40}Ca and ^{44}Ca, respectively. If this relatively weak fifth-order reflection is included in a real space analysis, the only difference profile that resembles that given in Fig. 3 *C* assumes $F(h = 5)$ has $\phi = \pi$ for DPPC with either ^{40}Ca or ^{44}Ca. When $\phi = 0$, the difference profile structure is physically unreasonable, containing high-frequency fluctuations throughout the difference profile, inconsistent with the profile structures in Figs. 2 and 3. The difference profile with $\phi = \pi$ for $F(h = 5)$ is shown in Fig. 4 *B* along with the corresponding neutron-scattering profile for ^{40}Ca-DPPC (Fig. 4 *A*). The fully resolved major maxima in this real space calcium difference profile are asymmetric and located 9.5 Å from the edge of the unit cell. The positions of these major maxima are similar to the positions of the major maxima (phospholipid head groups) in the neutron-scattering profile structure (compare Fig. 4 *A* with 4 *B*).

These interpretations of the real space difference profile are supported quantitatively by the more accurate reciprocal space analysis described by Buldt et al. (6). A reciprocal space model refinement of the difference structure factors for the two calcium isotopes, assuming a simple Gaussian model for the calcium distribution, yielded a 5.0 ± 1 Å wide ($1/e$ height Gaussian half-width) calcium binding strip located 6.0 ± 1.0 Å from the edge ($\pm d/2$) of the unit cell. The average positions of the major maxima within the real space difference calcium profiles (Figs. 3 *C* and 4 *B*) occur at 11.5 and 9.5 Å, respectively, from the edges ($\pm d/2$) of the unit cell. The position of the maxima within the real space difference profiles at successively higher resolution suggest that at sufficiently high resolution, the real space values may converge to the values

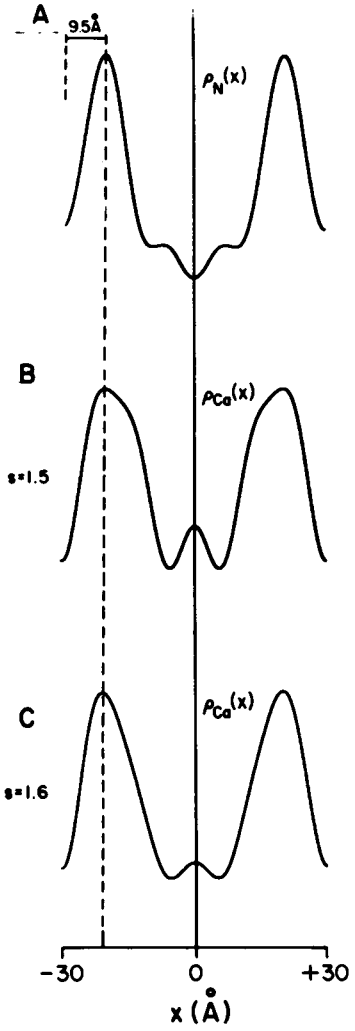

FIGURE 4 *A* is the neutron-scattering unit cell profile for the ^{40}Ca-DPPC multilayer in 100% H_2O using five diffraction orders. The calcium difference profile for DPPC bilayers in 5 mM added ^{40}Ca vs. ^{44}Ca for S = 1.5 is shown in *B* and for S = 1.6 is shown *C*. The temperature was 10°C. x represents the distance from the bilayer center in ångströms. Profiles are calculated as in Fig. 2 assuming a phase for the fifth-order equal to π.

obtained by the reciprocal space model refinement analysis operating on the first four diffraction orders as previously described (6–8). In addition, it has been shown that the reciprocal space analysis is less sensitive to the Gaussian half-width, in contrast to the average position of the peak density (6–8) so that the width of the calcium binding strip is known with less accuracy.

The results of Buldt et al. (6), who used deuterium-labeled DPPC in a neutron diffraction study, clearly defined the average position of the phosphate group of the DPPC head group along the profile axis. For DPPC in the $L_{\beta'}$ phase (~25% water content, d = 62.5 Å), which is similar to our study with DPPC (d = 61 Å, 20% water content), the phosphate groups were shown by Buldt et al. (6) to be located 7.7 Å from the edges ($\pm d/2$) of the DPPC/H_2O unit cell. The present findings indicate that calcium is localized at the average position of 6 Å from the edge ($\pm d/2$) of the DPPC/H_2O unit cell. If the 1.5-Å difference (which corresponds to 0.75 Å for the half-unit cell) in the unit cell repeats for these two studies is solely a result of the water layer thickness, our determination of the average location of calcium (6 Å from the edge of the unit cell) and the position of the phosphate group (7.0 Å from the edge of the corrected unit cell) determined by Buldt et al. (6) are within the error of the model refinement analysis in reciprocal space. Thus, the interaction of calcium with the zwitterionic phosphatidylcholine moiety may occur at the phosphate group as expected from a charge-charge interaction (see vertical arrows in the lower right of Fig. 5).

The most probable distribution of calcium is shown schematically in Fig. 5. In the lower portion of this figure, the peak distribution of water and calcium do not coincide because water concentration is highest at the edges of the unit cell, whereas calcium concentration is highest near the edges of the lipid bilayer itself. This can be understood as each unit cell contains a lipid layer hydrated with water layers in which pure water resides at the edges ($\pm d/2$) of the unit cell. Calcium ions, which are in solution within the water layer, might be expected to exhibit a concentration gradient along the x-axis of the water profile of Fig. 3 *B* if

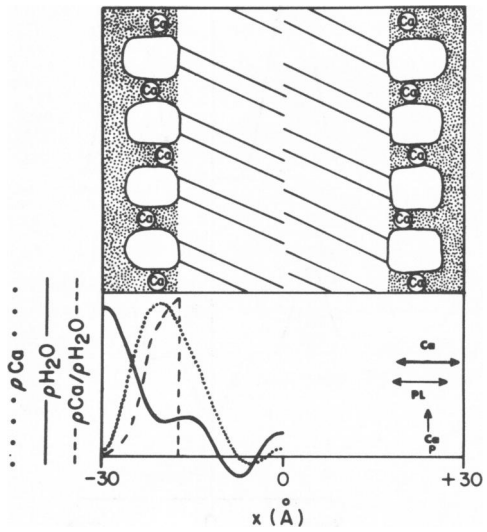

FIGURE 5 Calcium and water locations in a DPPC bilayer are schematically presented at 10°C and 66% relative humidity. The tilted lines represent crystalline ($L_{\beta'}$ phase) acyl chains that presumably exclude both calcium and water. Rounded, open rectangles represent phosphatidylcholine head groups whose average distributional width (full width at half maximum) derived from Fig. 3 *D*, is given by a horizontal vector PL in the *lower right*. The P vertical arrow represents the mean position of the phosphate group derived from Buldt et al. (6). Open circles containing "Ca" represent calcium ions either dissolved in water (stippled) or adsorbed to head groups. The calcium vector (horizontal) and vertical arrow at the *lower right*, derived from analysis (6, 7) of data given in this paper, represent the Gaussian half-width and mean position of calcium density. At the *lower left*, calcium density, water density, and their ratio are represented in relative units as derived from real space profiles.

preferential adsorption of calcium to the phosphate anion of the phosphatidylcholine head groups exists. Under the conditions reported in this study (10 mol phospholipid/mol calcium), it is likely that all of the available calcium is bound to the phospholipid head groups as supported by the calcium difference profiles of Figs. 3 *C* and 4 *B*.

This model in which calcium is bound to the phosphate moiety of the DPPC head groups, is appropriate for the specific conditions employed; namely, for low ionic strength and millimolar concentrations of calcium for the DPPC suspension and for partial hydration of the DPPC multilayer in which the concentrations of calcium and lipid are elevated. Under these conditions all the calcium present in the multilayer is apparently bound to the phosphate moiety of the DPPC head groups in a ratio of 1 mol calcium/10 mol DPPC. It is anticipated that for lipid suspensions with either low concentrations of calcium and/or high ionic strength, the molar ratio of calcium bound to the phosphate region may decrease and calcium may bind to other regions within the phospholipid head group. Nevertheless, physical arguments using electrostatic double-layer theory predict that the binding plane for divalent cations is 3.5 Å away from a hypothetical interface that separates water from lipid bilayers (3). It is physically reasonable to define this interface as the edge of the hydrocarbon region (i.e., the second carbon atom of the fatty acyl chains) of the DPPC bilayer (6–8). This is reasonable when the water profile structure (Fig. 3 *B*) is taken into account (see also 6, 7). Using previous neutron-diffraction results (6, 7) and the results obtained in this paper to locate calcium, the binding plane for calcium would then be ~4 Å away from this water/hydrocarbon interface, which agrees remarkablely with the predictions from electrostatic double-layer theory.

The interaction of divalent cations with model and biological membranes has been extensively studied with nuclear magnetic resonance (NMR) techniques. Using phosphorus NMR, calcium was shown to cause shifts in the phosphate peak corresponding to the head groups in the outer surface of the lipid bilayer vesicles (17, 18). However, this study was not directly conclusive regarding the location of calcium relative to the lipid bilayer structure. Another study observed calcium binding to DPPC by measuring its effect on the binding of Eu^3, using proton NMR to monitor the chemical shift in the proton $N(CH_3)_3$ signal (19). This approach allowed the binding constant for calcium to be determined and provided further evidence that calcium interacts somewhere within the DPPC head group. However, a study by McLaughlin et al. (1), using phosphorus NMR and cobalt to probe divalent cation-lipid interactions, provided strong evidence for the molecular site of divalent cation interaction with model lipid bilayers. Their conclusion was that the phosphate group was incorporated into the first coordination sphere of the cobalt ion. By inference, the calcium ion must also be close to the phosphate moiety of the DPPC head groups. The neutron diffraction approach presented in this paper provides a direct determination of this interaction that is in excellent agreement with the results of this latter NMR study.

The present report shows that neutron diffraction with calcium isotopes can be used to determine the distribution and location of calcium ions in lipid bilayers for ratios of 1 mol calcium/10 mol DPPC lipid. Experimentally, it appears to be feasible to locate 1 mol calcium/20–30 mol lipid using this model bilayer system where calcium binds to both monolayers of the DPPC bilayer. Although we have not attempted to place the calcium difference profile on an absolute scale to estimate calcium concentration along the profile axis, quantification of the molar ratio of calcium to lipid allows an interpretation of the neutron diffraction results in which the predominant interaction of calcium under the conditions of this study is with the phosphate moiety of the DPPC head groups. It is, therefore, attractive to apply this isotopic substitution technique to biological membranes containing high-affinity calcium binding sites to define the location of calcium binding sites on proteins. For example, we have recently prepared highly purified sarcoplasmic reticulum membranes (lipid-to-protein ratio ~100 mol lipid/mol calcium pump protein) with ^{40}Ca and ^{44}Ca bound only to the high-affinity binding sites following an EGTA treatment to remove additional calcium presumably bound nonspecifically to some of the phospholipid head groups of the membrane bilayer. Under these conditions, two moles calcium were bound per mole of calcium pump protein (or 1 mol calcium/50 mol lipid). These high-affinity sites for calcium in the sarcoplasmic reticulum membrane may be in close proximity to one another (20) so that, to a first approximation, they may be confined to a small extent along the profile axis of the sarcoplasmic reticulum membrane and be taken to represent a single site. Model calculations predict that, depending upon the position of the high-affinity bound calcium within the unit cell, neutron diffraction may be sufficiently sensitive for distinguishing whether the high-affinity calcium binding sites are localized somewhere in the protein knob region or the membrane bilayer region of the sarcoplasmic reticulum. It would then be of interest to compare the results of this approach to these obtained by alternative methods such as fluorescence energy transfer (21) or x-ray resonance scattering (22, 23). Because the structure of the calcium pump protein has been determined to some degree (8, 10, 12, 13), the location of these sites within the membrane may provide insight regarding the functional mechanism of calcium transport by this membrane system.

APPENDIX

Error-Limit Calculation for Experimental Structure Factors

The error limits for the structure factor moduli, $F(h)$, given in Tables I and II, were computed from the noise fluctuation observed in the intensity function, $I(s)$, over defined regions of reciprocal space where $s = 2\sin\theta/\lambda$.

The average noise per channel was computed near each discrete reflection, $I(h/d)$, where h is the reflection order index and d is the average multilayer unit cell repeat distance. For a given reflection, at h/d in reciprocal space, centered at the $h \cdot m^{th}$ channel, spread over $2b + 1$ channels, where b is the Gaussian $1/e$ half-width, the channel to channel noise, N, is:

$$N = \left(\sum_{k=1}^{k_{max}} \sum_{i=m(2h-1)/2}^{hm-b} |I(i) - I(i+k)| + \sum_{k=1}^{k_{max}} \sum_{i=hm+b}^{m(2h+1)/2} |I(i) - I(i+k)| \right) / \Delta, \quad \text{(A1)}$$

where Δ equals the total number of differences $|I(i) - I(i + k)|$ and normalizes the summation per channel. The allowable differences $|I(i) - I(i + k)|$ are bounded such that $i + k \leq hm - b$ for the first summation and $i + k \leq m(2h + 1)/2$ for the second summation. The average noise fluctuation per channel is thus given as $\pm N/2$. The total noise for an integrated reflection $I(h/d)$ is given as $(2b + 1) \cdot N/2$ and the structure factor limits are computed from $[(2b + 1) \cdot h/d \cdot N]/4\sqrt{\cdot h/d \cdot I(h/d)}$, where $F(h/d) \propto \sqrt{(h/d) \cdot I(h/d)}$ (24).

Model Calculations for Difference Structure Factors

This section of the Appendix provides calculations of difference structure factors as a function of the molar ratio of phospholipid to calcium. A step function model of the profile structure of the DPPC lipid bilayer with ^{40}Ca vs. ^{44}Ca bound to the phospholipid head group region was constructed. The methodology for such step function model calculations has been previously described (8, 25). The basic features of this profile structure are a 40-Å thick lipid bilayer, hydrated by protonated water with calcium bound to the phospholipid head group (see inset of Fig. 6). A step function model was constructed that contained five regions using the following scattering amplitude densities, ρ (cm/Å^3 × 10^{-14}), for the various membrane components: lipid head group, 1.6; hydrocarbon core, −0.3; water (H), −0.6; ^{40}Ca, 11.7; and ^{44}Ca, 4.5.

The calcium ion was defined as being confined to a 1-Å strip symmetrically placed in the phospholipid head group region. The density of this 1-Å strip was calculated from

$$\rho = \frac{N_L \rho_L + N_c \rho_c}{N_L + N_c}, \quad \text{(A2)}$$

where ρ_L and ρ_c are the scattering amplitude densities for the phospholipid head group and the calcium isotope, respectively. The ratio, $R = N_L/N_c$ is the molar ratio of phospholipid to calcium. Step function profile structure pairs were Fourier transformed and difference structure factors, $\Delta F_c(h)$, were calculated according to $[F_{^{40}Ca}(h) - F_{^{44}Ca}(h)]$ where h is the order index. Because the magnitude of the unit cell structure factors ($F_{^{40}Ca}$ and $F_{^{44}Ca}$) are model dependent, whereas the normalized difference structure factors are less so, a summation of the difference structure factors for various values of R were then calculated according to

$$\frac{\left| \sum_{h=1}^{h_{max}} \Delta F_c(h) \right|}{\left| \sum_{h=1}^{h_{max}} F_{^{44}Ca}(h) \right|}. \quad \text{(A3)}$$

The summation was computed for $h_{max} = 5$ because, experimentally, five orders were recorded and arbitrarily normalized to the sum of the structure factors for the step function model containing ^{44}Ca. The log of this normalized summation was then plotted as a function of the log R as given in Fig. 6.

The experimentally observed difference structure factors given in Table II were similarly normalized according to Eq. A3. This normalized sum, indicated by $\sum \Delta F_e$, intersects the calculated curve of Fig. 6 predicting a value of R = 11 mol phospholipid/mol calcium. The experimentally measured value of R as given in the Materials and Methods section is 10 ± 1 mol phospholipid/mol calcium. Therefore, the predicted value of R given by the model in Fig. 6 falls within the standard deviation of the experimentally measured value of R.

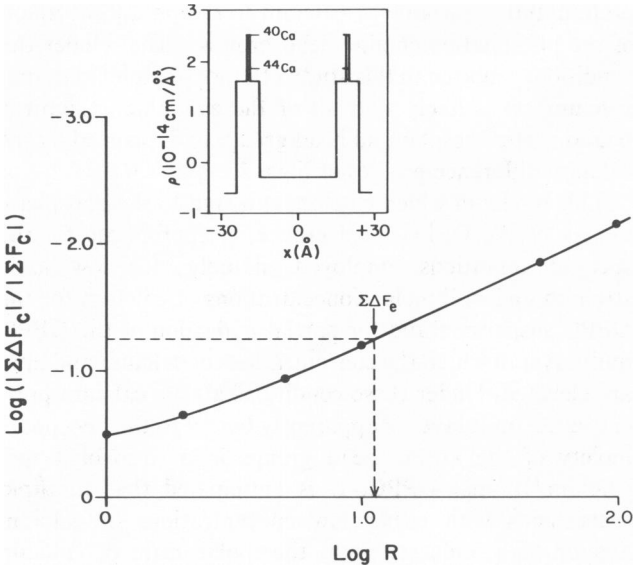

FIGURE 6 Model calculations of the difference structure factors as a function of the molar ratio of the calcium and phospholipid.

Even though such calculations as these are model dependent, it was found that for calcium bound to the phospholipid head group, the phase factors for the calculated difference structure factors were the same as those determined independently for the experimental difference structure factors. Models in which the calcium was placed within the hydrocarbon core region of the step-function model profile predicted values of R <8 or >30 and incorrect phases for the difference structure factors.

Dr. Herbette is a Charles E. Culpeper Foundation Fellow. We gratefully acknowledge the assistance of Dr. A. Suxena and Dr. B. P. Schoenborn at the Brookhaven National Laboratory.

The research was supported by research grants HL-21812, HL-22135, HL-26903, HL-27630, and HL-32588 from the National Institutes of Health and a grant from the American Heart Association. C. A. Napolitano and R. V. McDaniel's research was also supported by research training grant HL-07420 from the National Institutes of Health.

Received for publication 14 February 1984 and in final form 24 May 1984.

REFERENCES

1. McLaughlin, A. C., C. Grathwohl, and S. G. A. McLaughlin. 1978. The adsorption of divalent cations to phosphatidylcholine bilayer membranes. *Biochim. Biophys. Acta.* 513:338–357.
2. Inoko, Y., T. Yamaguchi, F. Furuya, and T. Mitsui. 1975. Effects of cations on dipalmitoylphosphatidylcholine/cholesterol/water systems. *Biochim. Biophys. Acta.* 413:24–32.
3. Lis, L. J., W. T. Lis, V. A. Parsegian, and R. P. Rand. 1981. Adsorption of divalent cations to a variety of phosphatidylcholine bilayers. *Biochemistry.* 20:1771–1777.
4. White, S. H., G. I. King, and J. E. Cain. 1981. Location of hexane in

lipid bilayers determined by neutron diffraction. *Nature (Lond.)*. 290:161–163.

5. Herbette, L., A. M. Katz, and J. Sturtevant. 1983. Comparison of the interaction of propranolol and timolol with model and biological membrane systems. *Mol. Pharmacol.* 24:259–269.
6. Buldt, G., H. U. Gally, J. Seelig, and R. Zaccai. 1979. Neutron diffraction studies on phosphatidylcholine model membranes. I. Head group conformation. *J. Mol. Biol.* 134:673–691.
7. Zaccai, G., G. Buldt, A. Seelig, and J. Seelig. 1979. Neutron diffraction studies on phosphatidylcholine model membranes. II. Chain conformation and segmental disorder. *J. Mol. Biol.* 134:693–706.
8. Herbette, L., A. Scarpa, J.K. Blasie, C. T. Wang, L. Hymel, J. Seelig, and S. Fleischer. 1983. Determination of the separate Ca^{2+} pump protein and phospholipid profile structures within reconstituted sarcoplasmic reticulum membranes via x-ray and neutron diffraction. *Biochim. Biophys. Acta.* 730:369–378.
9. Pachence, J. M., P. L. Dutton, and J. K. Blasie. 1981. The reaction center profile structure derived from neutron diffraction. *Biochim. Biophys. Acta.* 635:267–283.
10. Blasie, J. K., J. M. Pachence, and L. Herbette. 1984. Comment on the importance of appropriate neutron diffraction data in the decomposition of membrane scattering profiles into the separate scattering profile of their molecular components. *In* Basic Life Science. Vol. 27. Neutrons in Biology. B. P. Schoenborn, editor. Plenum Publishing Corp., New York. 27:201–210.
11. Bacon, G. E. 1962. Neutron Diffraction. Oxford University Press, Inc., New York.
12. Herbette, L., J. Marquardt, A. Scarpa, and J. K. Blasie. 1977. A direct analysis of lamellar x-ray diffraction from hydrated oriented multilayers of fully functional sarcoplasmic reticulum. *Biophys. J.* 20:245–272.
13. Herbette, L., C. T. Wang, A. Saito, S. Fleischer, A. Scarpa, and J. K. Blasie. 1981. Comparison of the profile structures of isolated and reconstituted sarcoplasmic reticulum membranes. *Biophys. J.* 36:47–72.
14. Moody, M. F. 1963. X-ray diffraction pattern of nerve myelin! A method for determining the phases. *Science (Wash. DC).* 142:1173–1174.
15. Stamatoff, J. B., and S. Krimm. 1976. Phase determination of x-ray reflections for membrane-type systems with constant fluid density. *Biophys. J.* 16:503–516.
16. Worthington, C. R., G. I. King, and T. J. McIntosh. 1973. Direct structure determination of multilayered membrane-type systems which contain fluid layers. *Biophys. J.* 13:480–494.
17. Grasdalen, H., L. E. G. Eriksson, J. Westman, and A. Ehrenberg. 1977. Surface potential effects on metal ion binding to phosphatidylcholine membranes. *Biochim. Biophys. Acta.* 469:151–162.
18. Hutton, W. C., P. L. Yeagle, and R. B. Martin. 1977. The interaction of lanthanide and calcium salts with phospholipid bilayer vesicles: the validity of the nuclear resonance method for determination of vesicle bilayer phospholipid surface ratios. *Chem. Phys. Lipids.* 19:225–265.
19. Hauser, H., C. C. Hinckley, J. Krebs, B. Levine, M. C. Phillips, and R. J. P. Williams. 1977. The interaction of ions with phosphatidylcholine bilayers. *Biochim. Biophys. Acta.* 468:364–377.
20. Highsmith, S. R. 1984. Distances between binding sites on SR CaATPase. *Biophys. J.* 45 (2, Pt. 2):4*a*. (Abstr.)
21. Scott, T. L. 1984. Luminescence studies of terbium bound to the Ca-ATPase of sarcoplasmic reticulum. *Biophys. J.* 45 (2, Pt. 2):3*a*. (Abstr.)
22. Stamatoff, J., P. Eisenberger, J. K. Blasie, J. Pachence, A. Tavormina, M. Erecinska, L. Dutton, and G. Brown. 1982. The location of redox centers in biological membranes determined by resonance x-ray diffraction. I. Observation of the resonance effect. *Biochim. Biophys. Acta.* 679:177–187.
23. Blasie, J. K., J. M. Pachence, A. Tauormina, M. Erecinska, P. L. Dutton, J. Stamatoff, P. Eisenberger, and G. Brown. 1982. The location of redox centers in biological membranes determined by resonance x-ray diffraction. II. Analysis of the resonance diffraction data. *Biochim. Biophys. Acta.* 679:188–197.
24. Bevington, P. R. 1969. Data Reduction and Error Analysis for the Physical Science. McGraw-Hill, Inc., New York. 56–64.
25. Pachence, J. M., P. L. Dutton, and J. K. Blasie. 1979. X-ray diffraction of reconstituted reaction center/lipid membranes. *Biochim. Biophys. Acta.* 548:348–373.